

## 2. Elastic Buckling of Columns

The present chapter is devoted to the basic concept of interest in stability of beam-columns. Analogies and differences with respect to the discrete systems utilized in the previous chapter for pointing out some basic definitions of equilibrium and stability will be also underlined.

### 2.1 Euler critical Load for beam-columns

A simply supported beam column can be firstly considered for determining the equilibrium configurations of more general continuous structures under axial load  $P$ , within the Euler hypotheses of small displacements and (and deformations) and perfect systems.

The beam represented in Figure 2.1 is in equilibrium when resting in the straight configuration; in this situation the axial force  $P$  only produces axial deformations  $\varepsilon = P/EA$ , being  $EA$  the axial stiffness of its cross section. Nevertheless, under the Euler hypotheses a further possible configuration is possible in the neighbours of the mentioned “trivial” one. Let this solution described be described by the law  $v(\xi)$ ; in the general cross section at the abscissa  $\xi$ , an external load  $M_{ext}$  arises and can be evaluated as follows:

$$M_{ext} = P \cdot v(\xi) . \quad (2.1)$$

Moreover, the internal moment  $M_{int}$  in the same cross section can be expressed in terms of the local curvature which is proportional to the second derivative of the deflection according to the well known equation reported below:

$$M_{int} = -EI \cdot v''(\xi) . \quad (2.2)$$

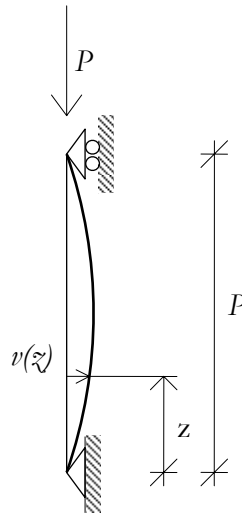


Figure 2.1: Simply supported beam with axial force  $P$ .

Equality between the two bending moments expressed by equations (2.1) and (2.2) is need for equilibrium and the following first order can be consequently obtained after few mathematical simplifications:

$$v''(\xi) + k^2 v(\xi) = 0 , \quad (2.3)$$

where  $k^2 = P/EI$ .

The second-order linear equation reported above can be solved according to several methods; since the discussion about the nature of solution depending upon the values of the coefficient  $k^2$  is of main concern, the above equation can be approached through the Fourier Series, taking account of the fact that any function defined within the range  $[0, L]$  can be expressed as series of sine and cosine functions. In particular, being the deflection of the beam in Figure 2.1 represented by an odd function

(namely, a function  $v$  in which  $v(\xi) = -v(-\xi)$  like whatever sine wave), it can be expressed in terms of sine series as follows:

$$v(\xi) = \sum_{n=1}^{\infty} v_n \sin \frac{n\pi\xi}{L} . \quad (2.4)$$

Since a series is basically a sum of (infinite) term, its derivatives can be easily determined as a sum of the derivatives of the various members. Consequently, the second derivative of  $v(\xi)$ , which is involved in equation (2.4), can be evaluated as follows:

$$v''(\xi) = -\sum_{n=1}^{\infty} \left( \frac{n\pi}{L} \right)^2 \cdot v_n \sin \frac{n\pi\xi}{L} . \quad (2.5)$$

The last two expressions assumed for the deflection function  $v(\xi)$  and its second derivative can be introduced in equation (2.3) obtaining the following relationships:

$$\sum_{n=1}^{\infty} \left[ k^2 - \left( \frac{n\pi}{L} \right)^2 \right] \cdot v_n \sin \frac{n\pi\xi}{L} = 0 . \quad (2.6)$$

Two possible kinds of solutions can be obtained by the above relationship:

- if  $v_n = 0$  for every value of  $n$ , the trivial solution is obtained, since all the coefficients of the series in equation (2.4) are null;
- if  $\left[ k^2 - \left( \frac{n\pi}{L} \right)^2 \right] = 0$ , then the corresponding coefficient  $v_n$  could be non-zero and the

deflection relationship described in equation (2.4) is different by the trivial one.

The latter condition occurs as

$$k^2 = \left( \frac{n\pi}{L} \right)^2 , \quad (2.7)$$

or, equivalently, as the axial load  $P$  achieves the following value:

$$P_{\sigma,n} = \frac{n^2 \pi^2 EI}{L^2} . \quad (2.8)$$

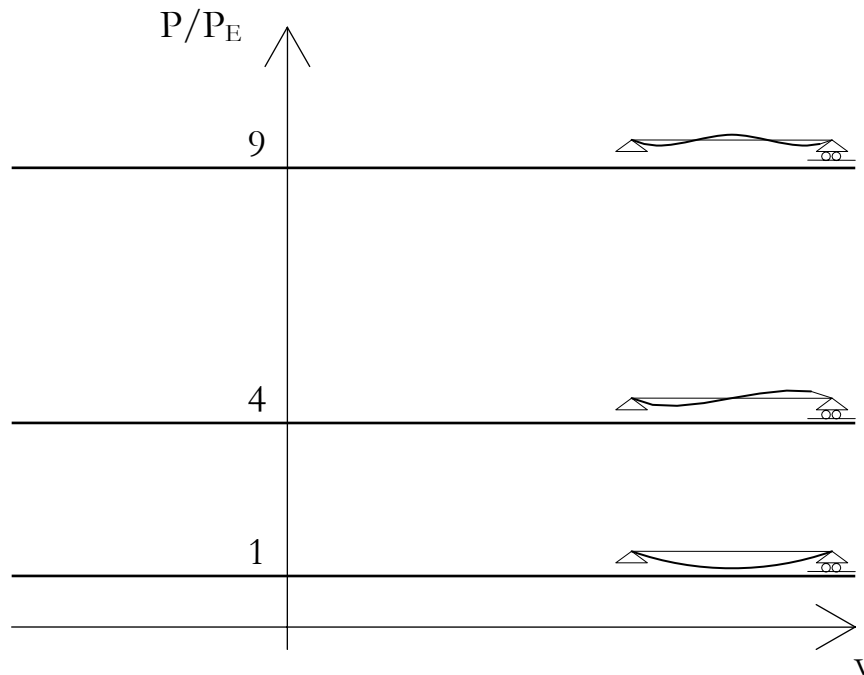


Figure 2.2: Critical loads and corresponding adjacent configurations of the beam.

Load values  $P_{\sigma,n}$  determined by equation (2.8) have the meaning of critical load in the Euler sense; as load  $P$  achieves that value a bifurcation in equilibrium path can occur. An infinite number of critical

loads  $P_{cr,n}$  can be theoretically determined according to the mathematical approach carried out above. Nevertheless, the smaller critical value, namely that obtained for  $n=1$ , for practical application is currently named the Euler critical load:

$$P_E = P_{cr,1} = \frac{\pi^2 EI}{L^2} . \quad (2.9)$$

The mechanical meaning of the above critical load can be easily understood by keeping in mind the theory developed in the previous chapter with reference to simple discrete systems. Since a finite number of kinematical parameters are needed for describing the behaviour of discrete systems, a finite number of critical loads can be obtained corresponding to different adjacent configurations in the neighbours of the trivial one. In particular, only one critical load value corresponding to the only possible adjacent configuration of the system has been found since the two discrete structures are basically single-degree-of-freedom systems. On the contrary, an infinite number of adjacent configurations can be found for general continuous systems, even those made out of a single elastic beams. Consequently, as a matter of principle, an infinite number of critical loads described by equation (2.8) can be found for the simply-supported beam considered above. Nevertheless, for the practical applications only the first one is usually of interest since bifurcation firstly occur under that load. Finally, equations (2.8) and (2.9) directly apply to simply-supported beams; in the next sections, the extension to whatever restraint condition will be exposed.

## 2.2 Magnification factor

Since structural members are often loaded even in transverse direction by a distributed load  $q(\xi)$  of general shape, its effect on stability needed to be investigated. Let  $v_0(\xi)$  be the deflection due to only the transverse load  $q(\xi)$  without considering the axial load  $P$ , and  $v(\xi)$  the total deflection taking account of both. First of all, the relationship between the bending moment  $M_0(\xi)$  due to  $q(\xi)$  and the corresponding deflection law  $v_0(\xi)$  is reported below:

$$M_0(\xi) = -EI v_0''(\xi) . \quad (2.10)$$

The expression of the external bending moment introduced by equation (2.1) has to be slightly modified for looking after the effect of bending moments induced by the transverse load:

$$M_{ext} = P \cdot v(\xi) + M_0(\xi) . \quad (2.11)$$

Consequently, the equilibrium condition between external and internal moments (the latter one always defined by equation (2.2)) results in the following second-order linear differential equation:

$$v''(\xi) + k^2 v(\xi) = v_0''(\xi) . \quad (2.12)$$

A solution procedure based on series development of both the initial (first-order, in the following) and complete deflections  $v_0(\xi)$  and  $v(\xi)$  can be utilized for solving the problem without précising the particular shape of the distributed load  $q(\xi)$ . In fact, for whatever distribution of transverse load an equivalent Fourier series can be introduced; under the hypotheses of load distribution symmetrical with respect to the mid-span point only sine-terms appears in that series:

$$v_0(\xi) = \sum_{n=1}^{\infty} v_{0,n} \sin \frac{n\pi\xi}{L} . \quad (2.13)$$

and the general expression of coefficients can be expressed as follows:

$$v_{0,n} = \frac{2}{L} \int_0^L v_0(\xi) \sin \frac{n\pi\xi}{L} \cdot d\xi . \quad (2.14)$$

Since the total deflection  $v(\xi)$  can be always developed through the Fourier series reported in equation (2.4), the differential equation (2.12) can be easily simplified as follows:

$$\sum_{n=1}^{\infty} \left[ \left( k^2 - \left( \frac{n\pi}{L} \right)^2 \right) \cdot v_n + \left( \frac{n\pi}{L} \right)^2 \cdot v_{0,n} \right] \cdot \sin \frac{n\pi\xi}{L} = 0 , \quad (2.15)$$

which is verified only if every value of the coefficient between square brackets is zero or, equivalently, under the following condition :

$$v_n = \frac{\left(\frac{n\pi}{L}\right)^2}{\left(\frac{n\pi}{L}\right)^2 - k^2} \cdot v_{0,n} = \frac{\left(\frac{n\pi}{L}\right)^2}{\left(\frac{n\pi}{L}\right)^2 - k^2} \cdot v_{0,n} = \frac{1}{1 - \frac{P}{P_{cr,n}}} \cdot v_{0,n} . \quad (2.16)$$

Making reference to the first term the following relationship can be pointed out:

$$\frac{v_1}{v_{0,1}} = \frac{1}{1 - \frac{P}{P_E}} . \quad (2.17)$$

meaning that the ratio between the coefficient of the first term of the series (2.4) and the corresponding one of the series in equation (2.13) are related to the critical load  $P_E$  through the expression on the right member of equation (2.17) which, consequently, assumes the meaning of magnification factor in the sense that total deflection ( $v(\xi)$  in equation (2.4)) can be obtained by amplifying the first order deflections ( $v_0(\xi)$  in equation (2.13)) according to that magnification factor.

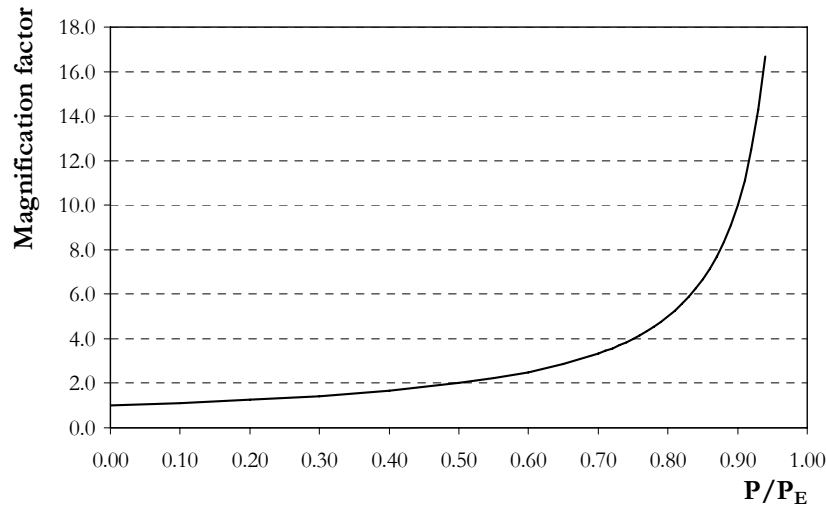


Figure 2.3: Magnification factor as a function of the critical load.

The same relationship can be easily recognised in the hypothesis that the two sine series in equation (2.4) and (2.13) are basically controlled by the corresponding first terms, resulting in the following approximate relationship:

$$\frac{v(\xi)}{v_0(\xi)} \approx \frac{v_1}{v_{0,1}} . \quad (2.18)$$

Consequently, the total-to-first-order ratio in terms of strain measures (namely, curvatures) can be even expressed in terms of the magnification factor defined in equation (2.16). Indeed, due to linear behaviour in terms of stress strain relationship, total bending moments  $M(\xi)$  can be even expressed in terms of the initial ones  $M_0(\xi)$ :

$$\frac{M(\xi)}{M_0(\xi)} = \frac{v_1''(\xi)}{v_{0,1}''(\xi)} \approx \frac{v_1}{v_{0,1}} . \quad (2.19)$$

Consequently, the following general expression can be assumed for evaluating the effect of axial forces on bending moments and, generally, on stresses in structures:

$$M(\xi) = \frac{1}{1 - \frac{P}{P_E}} \cdot M_0(\xi) . \quad (2.20)$$

The above equation and the definition of the magnification factor is often utilized for considering whether axial force affects or not the total stress and strain state of structures.

### 2.3 Theoretical classification of beam-columns

Equation (2.9) points out the value of axial load under which a possible bifurcation in equilibrium path; in other words, under the load  $P_E = P_{cr,1}$  a perfect (namely, perfectly straight and unaffected by accidental eccentricities) beam-columns, made out of an elastic material, two alternative equilibrium configurations are possible:

- The first one is the original straight (“trivial”) configuration which is admitted under whichever value of axial force P;
- The second one is a buckled configuration which can be approximated by a sine half-wave.

A critical stress can be easily evaluated through equation (2.9) dividing both members by the cross section area A:

$$\sigma_{cr} = \frac{\pi^2 E}{\lambda^2} . \tag{2.21}$$

Since real beam-columns, far from not being crooked, are surely made out of a material behaving elastically up to a limited value of stress  $f_y$  (i.e., the yielding stress in steel) a critical value of slenderness for which the critical stress defined by equation (2.21) is equal to the yielding stress  $f_y$  can be derived:

$$\lambda_p = \pi \sqrt{\frac{E}{f_y}} . \tag{2.22}$$

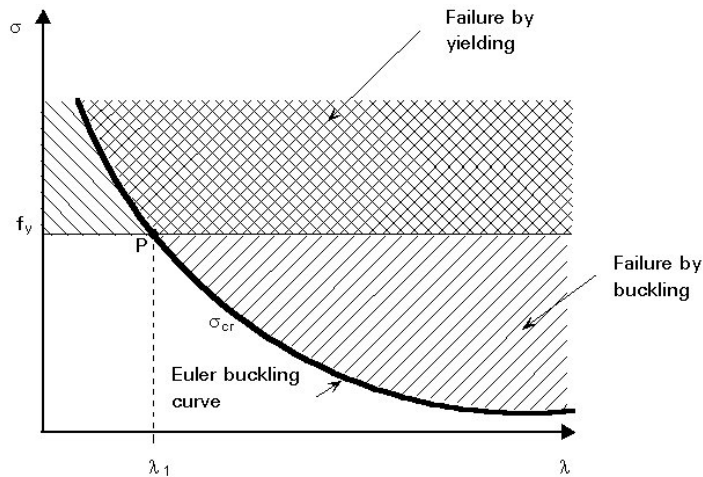


Figure 2.4: Axial strength of beam-columns as a function of slenderness.

Consequently, the overall field of slenderness can be subdivided into two main ranges:

- Stocky columns, for  $\lambda < \lambda_p$  in which yielding stress  $f_y$  is always greater than the critical stress resulting in buckling;
- Slender columns, for  $\lambda \geq \lambda_p$  which buckle within the elastic range since the critical stress is always smaller than the yielding stress.

### 2.4 The role of imperfection

Since geometrical imperfections, either in terms of lack in straightness in basic configuration or accidental eccentricity of loads, can be assumed as responsible for initial curvature of the beam-column, the equation (2.12) can be even utilized for describing the behaviour of members affected by an initial curvature (crookedness) due to imperfections rather than external transverse loads. The behaviour of imperfect systems with respect to the perfect one investigated in the light of Euler hypotheses has been already treated within the first chapter with reference to simple discrete systems: simple bifurcation have been pointed out for perfect ones, while asymptotical behaviour toward that bifurcation has been demonstrated for imperfect systems which experienced lateral deformations as large as the importance of imperfection.

Now, introducing the relative displacement  $w(z) = v(z) - v_0(z)$  the behaviour represented in Figure 2.5 can be intuitively understood, where the equilibrium path of columns is as far from the trivial configuration assumed by the perfect column for  $P < P_E$  as imperfection is relevant.

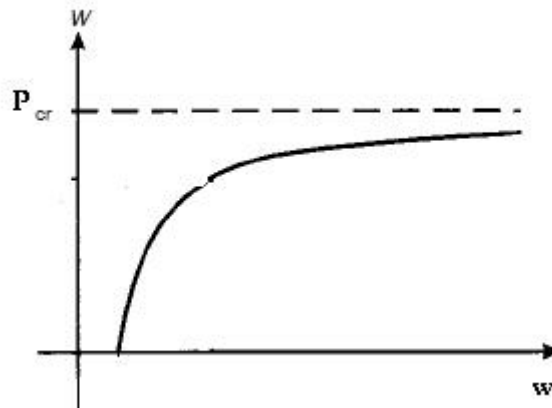


Figure 2.5: Behaviour of columns affected by initial curvature.

Since imperfection play a relevant role in affecting the equilibrium behaviour of beam-columns, an easy and reliable way for estimating its amount is needed. The definition of magnification factor reported in equation (2.17) can be proficiently utilised for evaluating the amplitude of imperfections, at least under the hypothesis of initial imperfection well approximated by the first term of the sine series in equation (2.14). In this case, equation (2.17) strictly applies and the following relationship in terms of relative displacement can be derived:

$$\frac{w}{P} = \frac{w}{P_E} + \frac{v_0}{P_E}, \quad (2.23)$$

relating the initial displacement  $v_0$  (namely the maximum deflection throughout the column axis due to imperfection) and the relative displacement  $w$ , which can be monitored during an experimental test through some displacement transducers placed along the column axis. Since the load  $P$ , can be applied and measured through load cells, the couples  $(w, w/P)$  can be plotted on a in the bidimensional graph: a straight line can be identified by means of a numerical regression and its slope can be related to the critical load as reported in Figure 2.6.

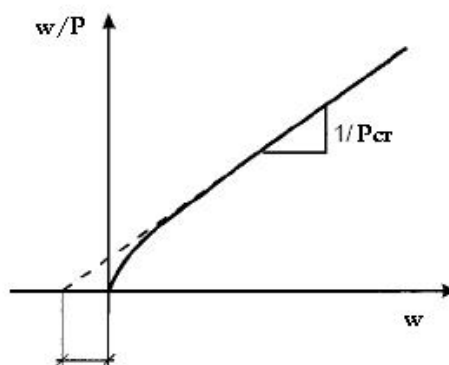


Figure 2.6: The "Southwell plot" for evaluating critical loads in imperfect columns.

## 2.5 Differential equation of beam-columns

The effect of axial force on elastic beam-column can be generally considered within the classical Bernoulli Theory for beams in bending which is basically founded upon the following two assumptions:

- Plane section remains plane after deformation;
- Deformed sections keep perpendicular to the (deformed) beams axis.

Under these hypotheses, the differential equations governing equilibrium can be easily derived obtaining the following two relationships:

$$dV + qdz = 0 \Rightarrow \frac{dV}{dz} + q = 0 , \quad (2.24)$$

$$dM - Vdz + qdz \cdot \frac{dz}{2} = 0 \Rightarrow \frac{dM}{dz} = V , \quad (2.25)$$

where  $M$  and  $V$  are the local bending and shear forces (Figure 2.7).

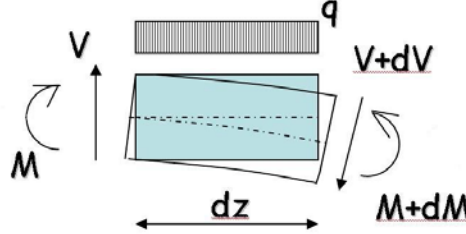


Figure 2.7: Equilibrium of an infinitesimal element without axial load effect.

The effect of axial force can be taken into account if the axial force is thought on the deformed configuration of the beam segment (Figure 2.8). Under this assumption equation (2.25) can be completed by considering the increase in moment due to axial load eccentricity  $dv$  evaluated with respect to the deformed shape of the beam-column:

$$dM - Vdz + qdz \cdot \frac{dz}{2} - P \cdot dv = 0 \Rightarrow \frac{dM}{dz} - P \frac{dv}{dz} = V , \quad (2.26)$$

where  $P$  is the axial (compressive) force.

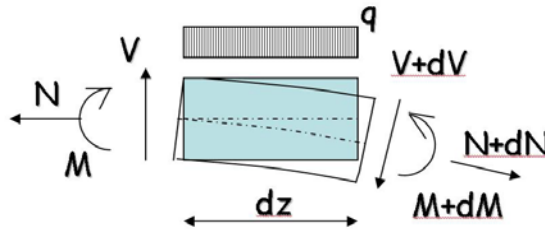


Figure 2.8: Equilibrium of an infinitesimal element with axial load effect.

Since the usual compatibility equations can be written between deflection  $v(z)$  and curvature, the following (generalized) stress-strain relation applies at least under the hypothesis of materials within the linear range:

$$M(z) = -EIv''(z) . \quad (2.27)$$

Finally, deriving once equation (2.26) and introducing equation (2.24) and, finally, deriving once more before of introducing equation (2.27) the following fourth-order differential equation with linear coefficients can be obtained:

$$v^{iv} + \frac{P}{EI}v'' = \frac{q}{EI} . \quad (2.28)$$

where two further hypotheses have been assumed:

- constant axial load  $P$  throughout the column axis;
- uniform value of the flexural stiffness  $EI$ .

In the cases of strictly positive (namely, compressive) axial load  $P$  the following definition can be introduced:

$$k^2 = \frac{P}{EI} , \quad (2.29)$$

and the general solution of equation (2.28) can be placed in the following form:

$$v(z) = A \sin kz + B \cos kz + Cz + D + v_p(z) , \quad (2.30)$$

where  $v_p(z)$  is a particular solution depending on the transverse load applied upon the beam.

The following equation can be utilized for determining the behaviour of beam-columns with axial load up to possibly deriving the critical value defined in the first paragraph of the present chapter. For instance, the behaviour of the simply supported beam-columns represented in Figure 2.1 can be studied providing equation (2.30) (in which  $v_p(\xi)=0$  since no transverse load is applied) with the relevant boundary conditions imposed by end restraints:

- for  $\xi=0$ :

$$\begin{aligned} v(0) &= 0 \\ M(0) = 0 &\Rightarrow v''(0) = 0 \end{aligned} \quad (2.31)$$

- for  $\xi=L$ :

$$\begin{aligned} v(L) &= 0 \\ M(L) = 0 &\Rightarrow v''(L) = 0 \end{aligned} \quad (2.32)$$

The above boundary conditions can be written in the following matrix form by pointing out some significant algebraic properties:

$$\begin{bmatrix} 0 & 1 & 0 & 1 \\ 0 & -k^2 & 0 & 0 \\ \sin kL & \cos kL & L & 1 \\ -k^2 \sin kL & -k^2 \cos kL & 0 & 0 \end{bmatrix} \cdot \begin{bmatrix} A \\ B \\ C \\ D \end{bmatrix} = \begin{bmatrix} 0 \\ 0 \\ 0 \\ 0 \end{bmatrix}. \quad (2.33)$$

The above set of simultaneous equations has the trivial solution ( $A=B=C=D=0$ ) as unique possible solution if the matrix is non singular. On the contrary, other possible solutions are admissible if the matrix determinant vanishes:

$$-k^4 L \sin kL = 0, \quad (2.34)$$

which is true if

$$kL = n\pi \quad \text{with } n \geq 1 \quad (2.35)$$

and, equivalently, if

$$\frac{P}{EI} = \frac{n^2 \pi^2}{L^2} \quad (2.36)$$

Equation (2.36) confirms that an infinite number of alternative equilibrium positions, stemming out by bifurcation at given values of the axial load  $P=P_{cr,n}$ , are possible. If the first one is of interest, Euler load  $P_E$  defined by equation (2.9) can be found out by equation (2.36) and a different and more general approach to evaluating critical loads in elastic beam-columns can be put in place by means of the differential equation of beam-columns under axial loads whose general solution is reported in equation (2.30).

## 2.6 Critical loads of perfect columns with various end-restraint

Evaluating critical loads of elastic beam-columns considering different end-restraint conditions can be pursued by introducing suitable boundary conditions instead of those written in eqs. (2.31) and (2.32) for simply-supported beams. For instance, the structural schemes reproduced in Figure 2.9 could be easily solved as described in the previous section. The first one, for example, which is fixed at one end and clamped at the other one could be solved by introducing the following boundary conditions:

- for  $\xi=0$ :

$$\begin{aligned} v(0) &= 0 \\ v'(0) &= 0 \end{aligned} \quad (2.37)$$

- for  $\xi=L$ :

$$\begin{aligned} v(L) &= 0 \\ M(L) = 0 &\Rightarrow v''(L) = 0 \end{aligned} \quad (2.38)$$

resulting in a set of simultaneous equations whose matrix of coefficient is singular if its determinant vanishes as described by the following equation:

$$\tan kL = kL. \quad (2.39)$$

The above equation can only be solved through numerical or graphical methods providing the following solution, among other grater ones:

$$kL \approx 4.4934 \approx 1.4303\pi , \tag{2.40}$$

and the following expression can be found for the critical load value:

$$P_E = \frac{\pi^2 EI}{(0.699 \cdot L)^2} . \tag{2.41}$$

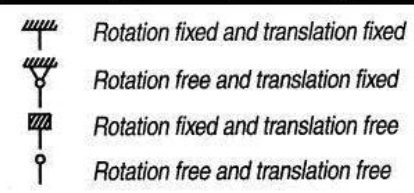
Buckled shape of column is shown by dashed line	(a)	(b)	(c)	(d)	(e)	(f)
Theoretical $\beta$ Value	0.5	0.7	1.0	1.0	2.0	2.0
Recommended design value when ideal condition are approximated	0.65	0.80	1.2	1.0	2.10	2.0
End Condition code						

Figure 2.9: Effective length  $L_0$  of columns with various end restraints.

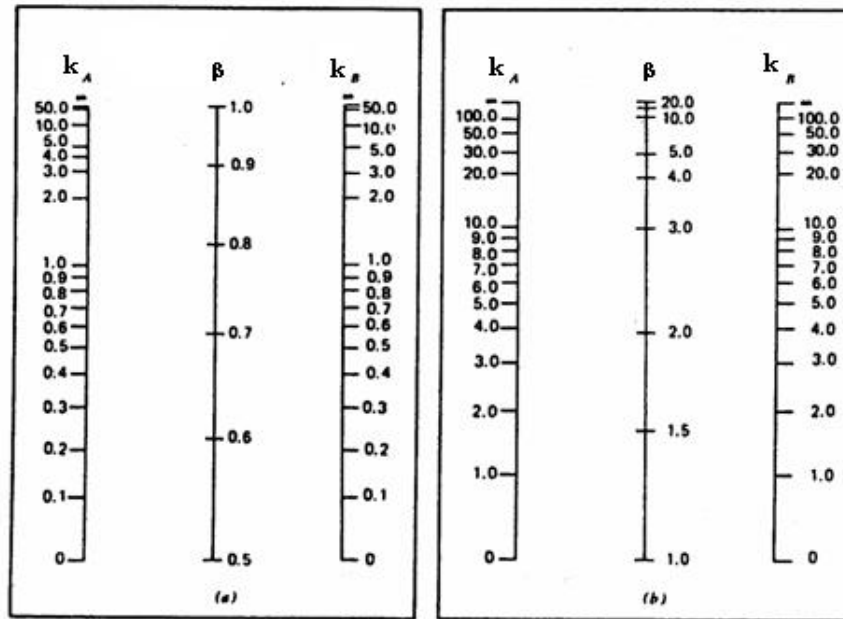
It is possible to demonstrate that the reduced span length at the denominator of the previous formula is the distance between the two zero-bending points, namely the one in which curvature is zero in the deformed configuration represented in Figure 2.9 and the clamped end of the beam. Based on this observation a general way for deriving the critical value  $P_E = P_{cr,1}$  of beam-columns under whichever restraint condition can be obtained by extending equation (2.9) by replacing the physical length  $L$  with the effective length  $L_0$  of the beam-column which bends as an half sine-wave in the adjacent equilibrium condition. In particular, a coefficient  $\beta$  can be introduced as a ratio between  $L$  and  $L_0$ :

$$L_0 = \beta L , \tag{2.42}$$

and the following general expression of the Euler load can be introduced:

$$P_E = \frac{\pi^2 EI}{L_0^2} . \tag{2.43}$$

Finally, in a more general sense, critical loads of beam-columns with flexible end restraints can be evaluated depending upon flexibility of such restraints. Although analytical solution of the problem is always possible, a more general and handy way for determining the values of  $L_0$  can be undertaken by using the so-called alignment charts or nomograms. Figure 2.10 reports to different alignment-charts related to non-say and sway systems, namely those in which relative transverse displacement of the two ends are restrained or allowed (non-sway or sway structures).



a) non-sway members

b) sway members

Figure 2.10: Alignment charts for beam-columns with flexible end restraints.

In both cases the input data are the non-dimensional beam end-flexibilities  $k_A$  and  $k_B$  and the corresponding value of the coefficient  $\beta$  can be easily derived as the intersection between the aligning straight line and the central axis. Considering non-sway schemes, coefficient  $\beta$  values ranges between 0.50 and 1.0 as the end restraints range from completely stiff ( $k_A = k_B = 0$ ) to completely deformable ( $k_A \rightarrow \infty, k_B \rightarrow \infty$ ). On the contrary, for the same flexibility values, coefficient  $\beta$  in sway columns ranges from 1.0 to infinity.

The effective length or the coefficient  $\beta$  can be alternatively determined according to the following analytical relationships:

- non-sway members:

$$\beta = 0.5 \cdot \sqrt{\left(1 + \frac{k_A}{0.45 + k_A}\right) \cdot \left(1 + \frac{k_B}{0.45 + k_B}\right)}, \quad (2.44)$$

- sway members:

$$\beta = \max \left\{ \sqrt{1 + 10 \frac{k_A k_B}{k_A + k_B}}; \left(1 + \frac{k_A}{1 + k_A}\right) \cdot \left(1 + \frac{k_B}{1 + k_B}\right) \right\}. \quad (2.45)$$

Other possible approximate expressions for the  $\beta$  coefficient can be found within the scientific and technical literature, in terms of the nodal flexibilities (or stiffnesses). Column end flexibility can be easily determined in the case of single members (Figure 2.11); the conceptual definition of nodal flexibility  $\varepsilon_i$  can be expressed as the ratio between the observed nodal rotation  $\theta_i$  and the applied moment  $M_i$ :

$$\varepsilon_i = \frac{\theta_i}{M_i}. \quad (2.46)$$

In other words the nodal flexibility is the nodal rotation obtained for a unit nodal moment. The relative flexibility coefficient  $k_i$  to be used for deriving the  $\beta$  coefficient through the alignment charts in Figure 2.10 or the approximate relationships (2.44) and (2.45) is defined by dividing such nodal flexibility by a term related to the column flexural deformability:

$$k_i = \frac{\varepsilon_i}{L_{col} / EI_{col}}. \quad (2.47)$$

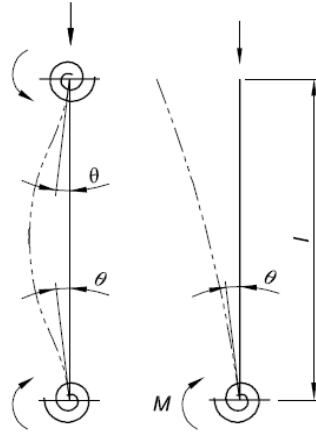


Figure 2.11: Definition of nodal flexibility for single members.

Furthermore, both the alignment charts and the mentioned approximate relationships can be used for the more general task of defining the effective length and the  $\beta$  coefficient for a beam-column in a general frame. According to the symbols briefly introduced in Figure 2.15 the relative flexibility terms  $k_A$  and  $k_B$  can be derived as follows:

$$k_A = \frac{\varepsilon_A + L_{col,1} / EI_{col,1}}{L_{col,1} / EI_{col,1} + L_{beam,11} / EI_{beam,11} + L_{beam,12} / EI_{beam,12}} \quad (2.48)$$

$$k_B = \frac{\varepsilon_B + L_{col,2} / EI_{col,2}}{L_{col,2} / EI_{col,2} + L_{beam,21} / EI_{beam,21} + L_{beam,22} / EI_{beam,22}} \quad (2.49)$$

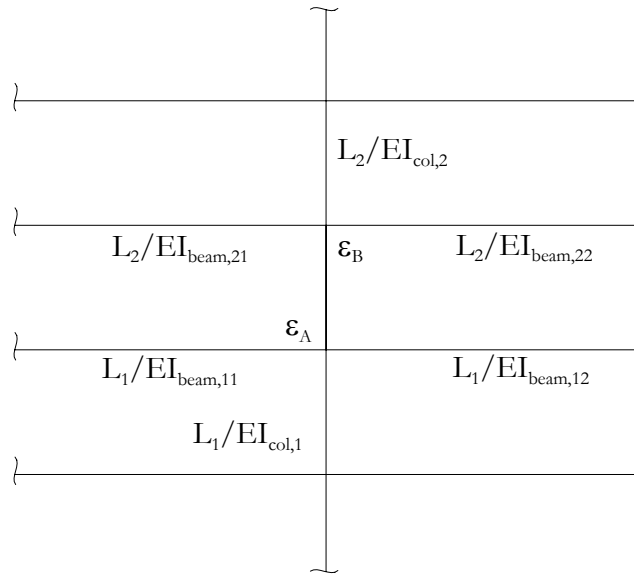


Figure 2.12: Definition of nodal flexibility for a member in frame.

## 2.7 Role of shear flexibility on stability of beam-columns

Shear flexibility is usually neglected especially when slender members are considered. Nevertheless, at least under a theoretical point of view, shear flexibility affects stability of members and structures as can be easily demonstrated in the following. Coming back to the assumptions of the first chapter, equation (2.1) generally applies, while equation (2.2) has to be updated to take into account the deformation contribution due to shear flexibility. Since it basically consists of a shear strain  $\gamma$  which is as great a shear force  $V$ , the following relationship can be introduced:

$$\gamma = \frac{\chi_V}{GA} \cdot V \quad (2.50)$$

where  $\chi_V$  is the shear factor of the transverse section,  $G$  is the shear elastic modulus and  $\mathcal{A}$  the cross section area.

Consequently, shear strain results substantially results in an increase in beam curvature  $\chi$  which can be evaluated as the second derivative of  $\gamma$ :

$$\chi = \frac{d\varphi}{dz} = -\frac{d^2v}{dz^2} + \frac{d\gamma}{dz} = \frac{M}{EI} , \quad (2.51)$$

and the following definition of the bending moment as a function of flexural and shear strains can be obtained to replace equation (2.2):

$$M_{\text{int}} = -EI \left[ \frac{d^2v}{dz^2} - \chi_V \cdot \frac{V'}{GA} \right] . \quad (2.52)$$

Since shear force  $V$  is the first derivative of the bending moment  $M$ , the following relationship can be stated:

$$V' = M'' = \frac{d}{dz}(Pv) = Pv'' . \quad (2.53)$$

which can be substituted in equation (2.52) with aim of expressing the (internal) bending moment as a function of the second derivative of deflection function  $v(z)$ :

$$M_{\text{int}} = -EI \left[ 1 - \chi_V \cdot \frac{P}{GA} \right] \frac{d^2v}{dz^2} . \quad (2.54)$$

If the second members of equation (2.1) and (2.54) are equal, as required by equilibrium, the following second order differential equation can be derived instead of equation (2.3):

$$\frac{d^2v}{dz^2} + \frac{P}{EI \left[ 1 - \chi_V \cdot \frac{P}{GA} \right]} \cdot v = 0 . \quad (2.55)$$

A new expression of the critical load  $P_{cr}$  can be derived under the same hypotheses mentioned in the first paragraph where only flexural strains have been considered:

$$\frac{P_{cr,V}}{EI \left[ 1 - \chi_V \cdot \frac{P_{cr,V}}{GA} \right]} = \left( \frac{\pi}{L_0} \right)^2 , \quad (2.56)$$

and

$$P_{cr,V} = \frac{\pi^2 EI}{L_0^2} \cdot \frac{1}{1 + \frac{\pi^2}{L_0^2} \cdot \chi_V \cdot \frac{EI}{GA}} = P_{cr} \cdot \frac{1}{1 + \frac{\pi^2}{L_0^2} \cdot \chi_V \cdot \frac{EI}{GA}} . \quad (2.57)$$

An alternative relationship for the critical load  $P_{cr,V}$  can be placed in the following form:

$$\frac{1}{P_{cr,V}} = \frac{1}{P_{cr}} + \frac{\chi_V}{GA} . \quad (2.58)$$

Finally, it is worth noticing that shear flexibility results in a reduction of the theoretical value of the critical load determined in the first paragraph for the Bernoulli beam. Such reduction is usually negligible for the most common simple profile, while can be relevant in built-up columns (namely, columns made out of angle or channel profiles assembled one another through braces or other members) as will be exposed in the following.

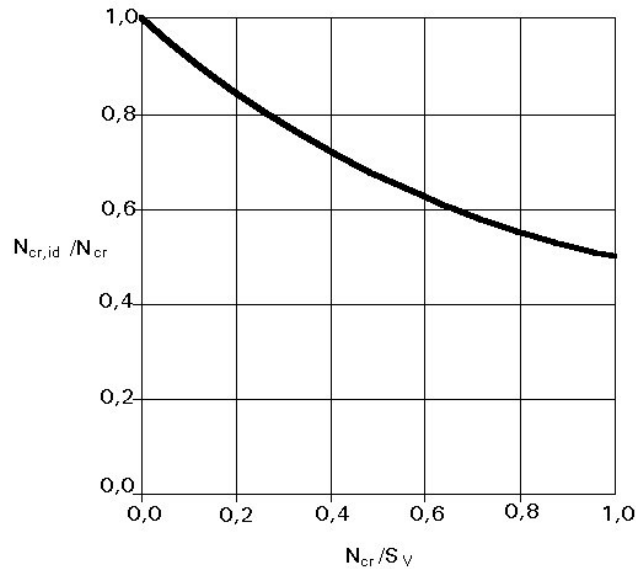


Figure 2.13: Reduction in critical load due to shear flexibility.

## 2.8 Code specifications for beam columns

Code provisions on stability of beam-columns can be regarded under the light of the general theoretical bases outlined within the previous sections whose contents are a fundamental background for whatever design-oriented discussion on stability of members and structures.

In the present paragraph the basic provisions of two codes of standards of interest for designers mainly working in Italy and Europe will be described and commented with reference to the key aspects related to stability checks of steel members. Indeed, the basic provisions of both the Italian Code (D.M. 96 [12]) and the European one (Eurocode 3, [13] and [14]) will be analyzed.

Global stability will be basically discussed even if some insights above local buckling possibly affecting steel members will be even addressed with particular reference to the main rules provided by Eurocode 3.

### 2.8.1 Stability check of beam-columns according to the Italian Code

The Code of Standard usually adopted in Italy is the D.M. 96 which allows the designers to adopt either the Permissible Stress Method or the Limit States Methods. The latter choice will be only considered in the following, although the use of the former one is still very popular among the Italian designers. The usual equation of safety checks according to Limit States Method can be consequently introduced as the design value of stresses  $S_d$  should not be greater than the corresponding design value of Resistance  $R_d$ :

$$S_d \leq R_d . \quad (2.59)$$

Stability check is one of the possible Ultimate Limit Verifications to be carried out on structures. Design values of stresses have to be derived by analyzing the structure under the design forces obtained by the well-known combination of permanent (self weights  $G_k$  and permanent loads  $G_k'$ ) and live actions  $Q_k$ :

$$F_d = \gamma_g \cdot (G_k + G_k') + \gamma_q \cdot \left[ Q_{k1} + \sum_{i=2}^n \psi_{0i} Q_{ki} \right] . \quad (2.60)$$

Resistance  $R_d$  can be generally evaluated with reference to the design values of material strengths; in particular, yielding stress  $f_{yk}$  is the mechanical properties of key importance for steel structures and the design value can be obtained as a function of the characteristic one through the definition of the partial safety factors  $\gamma_m$ :

$$f_{ad} = \frac{f_{yk}}{\gamma_m} . \quad (2.61)$$

Two possible ways can be followed for evaluating the design strength  $R_d$  of members as a function of material properties  $f_{ad}$ :

- plastic analysis of cross section could be carried out for deriving the ultimate (plastic) bending moment of members as follows:

$$M_{Rd} = W_{pl} f_{ad} ; \quad (2.62)$$

- conventional elastic analysis of cross section could be even carried out for evaluating the ultimate (plastic) bending moment of members:

$$M_{Rd} = W_{el} f_{ad} ; \quad (2.63)$$

Since the plastic modulus  $W_{pl}$  is always greater than elastic one  $W_{el}$ , the two definitions of (flexural) strength stemming by equations (2.62) and (2.63) will not be self-consistent. Consequently, the Italian code states that different values of the partial safety factor have to be considered when plastic or elastic analysis of section is carried out. In particular,  $\gamma_m = 1.12$  must be considered for plastic hypothesis (equation (2.62)), while a unit value of  $\gamma_m$  can be taken in equation (2.63). In this way, being 1.12 the approximate value of plastic-to-elastic modulus ratio for I-shaped profiles the two equations provide the same value at least for those sections which are the most widely used steel ones.

Stability check is one of the key steps for steel members according to the present code and it is carried out according to the well-known Omega-Method, theoretically described in section 2.3. Although the value of  $\omega$  is basically related to the column slenderness, it is also affected by the amount of imperfections deriving by the production and mounting process. Four different relationships (*curves*, in the following) are defined between the  $\omega$  factor and the corresponding slenderness  $\lambda$ , depending on the kind of profile of interest (and, consequently, the expected amount of imperfections):

- curve a, for single members of hollow square, rectangular or circular shape, welded or hot-rolled, whose maximum thickness is not greater than 40 mm;
- curve b: for simple members made out of I-shaped wide flange profiles whose height-to-width ratio is not smaller than 1.2 and thickness not greater than 40 mm (basically all IPE profiles, HEA starting from HEA400, HEB starting from HEB360 and HEM from HEM340). Furthermore, I-shaped profiles strengthened by welded planes and closed-section welded profiles, both thinner than 40 mm, follows this curve ;
- curve c: for simple or built-up members was thickness is not greater than 40 mm;
- curve d: all the sections thicker than 40 (i.e. the so-called *jumbo profiles*).

Finally, the  $\omega$  factor can be derived for each kind of profile depending on slenderness and according to the above classification; curves are different for the three possible steel grades (S235, S275, S355). The values in terms of non-dimensional slenderness and for the four curves mentioned above are reported in Table 2.1.

### 2.8.1.1 Stability check under axial load

Stability check under axial load  $N$  can be carried out by verifying that the given member complies with the following relationship given in terms of stresses:

$$\sigma_a = \frac{\omega N}{A} \leq f_{ad} , \quad (2.64)$$

where  $N$  is the axial force and  $A$  is the cross section area. Since two values of the second moment of inertia  $I_x$  and  $I_y$  (and, correspondingly, two values of the radius of gyration  $\rho_x$  and  $\rho_y$ ) can be defined around the two principal axes of the cross section, the maximum value of slenderness has to be considered:

$$\lambda = \max \left( \frac{L_{0,x}}{\rho_x} ; \frac{L_{0,y}}{\rho_y} \right) , \quad (2.65)$$

with the purpose of determining the relevant value of the  $\omega$  factor:

$$\omega = \omega(\lambda; \text{Stability curve}, \text{Steel grade}) . \quad (2.66)$$

Table 2.1: Values of the  $w$  factor as a function of the non-dimensional slenderness  $\lambda/\lambda_p$ .

$\lambda/\lambda_p$	$\sigma_c/f_d$				$\omega$			
	curve				curve			
	$a$	$b$	$c$	$d$	$a$	$b$	$c$	$d$
0,0	1,000	1,000	1,000	1,000	1,000	1,000	1,000	1,000
0,1	1,000	1,000	1,000	1,000	1,000	1,000	1,000	1,000
0,2	1,000	1,000	1,000	1,000	1,000	1,000	1,000	1,000
0,3	0,978	0,965	0,951	0,917	1,022	1,036	1,052	1,091
0,4	0,953	0,925	0,900	0,841	1,049	1,081	1,111	1,189
0,5	0,923	0,885	0,843	0,769	1,083	1,130	1,186	1,300
0,6	0,885	0,838	0,783	0,699	1,130	1,193	1,277	1,431
0,7	0,844	0,785	0,719	0,633	1,185	1,274	1,391	1,580
0,8	0,796	0,727	0,655	0,572	1,256	1,376	1,527	1,748
0,9	0,739	0,663	0,593	0,517	1,353	1,508	1,686	1,934
1,0	0,674	0,599	0,537	0,468	1,484	1,669	1,862	2,137
1,1	0,606	0,538	0,486	0,424	1,650	1,859	2,057	2,358
1,2	0,540	0,481	0,439	0,385	1,852	2,079	2,278	2,597
1,3	0,480	0,429	0,395	0,350	2,083	2,331	2,532	2,857
1,4	0,427	0,383	0,357	0,319	2,342	2,611	2,801	3,135
1,5	0,381	0,343	0,323	0,290	2,625	2,915	3,096	3,448
1,6	0,341	0,308	0,293	0,265	2,933	3,247	3,413	3,774
1,7	0,306	0,277	0,266	0,242	3,268	3,610	3,759	4,132
1,8	0,277	0,250	0,241	0,222	3,610	4,000	4,149	4,505
1,9	0,251	0,226	0,219	0,204	3,984	4,425	4,566	4,902
2,0	0,228	0,205	0,200	0,188	4,386	4,878	5,000	5,319
2,1	0,208	0,188	0,183	0,173	4,808	5,419	5,464	5,780
2,2	0,190	0,173	0,169	0,160	5,263	5,780	5,917	6,250
2,3	0,175	0,159	0,158	0,148	5,714	6,289	6,329	6,757
2,4	0,162	0,147	0,147	0,138	6,173	6,803	6,803	7,246
2,5	0,149	0,137	0,137	0,129	6,711	7,299	7,299	7,752
2,6	0,138	0,128	0,128	0,120	7,246	7,813	7,813	8,333
2,7	0,128	0,119	0,119	0,112	7,813	8,403	8,403	8,929
2,8	0,119	0,110	0,110	0,105	8,403	9,091	9,091	9,524
2,9	0,112	0,103	0,103	0,098	8,929	9,709	9,709	10,204
3,0	0,105	0,096	0,096	0,092	9,524	10,417	10,417	10,870

### 2.8.1.2 Stability check under eccentric axial load

Eccentricity hugely affects both strength and stability checks in steel members and the validity of the following relationship has to be verified for the member not to fail in buckling:

$$\sigma_a = \frac{\omega N}{A} + \frac{M_{eq,x}}{\psi_x W_{el,x} \left(1 - \frac{N}{N_{cr,x}}\right)} + \frac{M_{eq,y}}{\psi_y W_{el,y} \left(1 - \frac{N}{N_{cr,y}}\right)} \leq f_{ad} \quad (2.67)$$

where bending moments  $M_x$  and  $M_y$  around the two principal axes of inertia of the section are involved through an equivalent value whose meaning will be better explained in the following; magnification factors also appear for amplifying the stress contributions of bending moments and the two terms denoted as  $\psi_x$  and  $\psi_y$  are named “plastic adaptation coefficient” and can be conservatively placed to one for the sake of simplicity.

The two values of the critical loads in  $x$  and  $y$  directions can be easily evaluated as a function of the geometrical properties of the column and its cross section:

$$N_{cr,x} = \frac{\pi^2 EI_x}{L_{0,x}^2}, \quad N_{cr,y} = \frac{\pi^2 EI_y}{L_{0,y}^2}. \quad (2.68)$$

Finally, the meaning of the equivalent bending moments  $M_{eq}$  needs to be clarified as a function of the shape of the corresponding diagram. First of all, equivalent bending moment  $M_{eq} = M_0$  as an uniform bending moment diagram is considered. Secondly the following relationship can be considered among the equivalent value and the two nodal ones  $M_a$  and  $M_b$ , being  $|M_a| \geq |M_b|$ :

$$M_{eq} = 0.6M_a - 0.4M_b \geq 0.4M_a. \quad (2.69)$$

Finally, in a more general case of non linear (i.e. parabolic) shape of the bending moment diagram the equivalent bending moment can be determined as follows:

$$M_{eq} = 1.3M_m. \quad (2.70)$$

$M_m$  being the average value of bending moment throughout the column axis and always considering the following limitation:

$$0.75M_{\max} \leq M_{eq} \leq M_{\max}. \quad (2.71)$$

## 2.8.2 Stability check of beam-columns according to Eurocode 3

A more general approach to stability of beam-columns is pursued in Eurocode 3 in which a clear difference is firstly stated among steel members depending on the geometric and mechanical properties of their cross section. Consequently, steel profiles are divided into four different classes with respect to their ultimate behaviour in terms of both (flexural) strength and ductility. The first of the following subsections will explain with enough details this issue, while the other two will deal with the stability check of members under axial load with or without eccentricity.

Finally, it is worth noticing that safety checks in EC3 are formulated within the general framework of the Limit States Methods. Consequently, stability check deals with the Ultimate Limit State of the member and the action can be combined according to a rule like the one reported by equation (2.60). Similar formula can be even assumed for defining the design strength of material, but a more complicated way of defining the value of partial safety factor is considered in EC3, in which a different value has to be taken into account depending on the kind of failure mechanism of concern. Precisely, a value  $\gamma_{M1} = 1.05$  can be assumed for Stability while all the other possible values of the safety factors are reported in Table 2.2 for the sake of completeness.

Table 2.2: Values of the safety factors according to EC3.

LIMIT STATE	SUBJECT	SAFETY FACTORS
MATERIALE	Elastic limit state of the section	$\gamma_M = 1.00$
	Plastic collapse of the structure	$\gamma_M = 1.12$
	Transverse section in Class 1, 2, 3	$\gamma_{M0} = 1.05$
	Transverse section in Class 4	$\gamma_{M1} = 1.05$
	Stability of members	$\gamma_{M1} = 1.05$
	Strength of net section	$\gamma_{M2} = 1.20$
JOINTS	Bolts	$\gamma_{Mb} = 1.35$
	Rivets	$\gamma_{Mr} = 1.35$
	Pivots	$\gamma_{Mp} = 1.35$
	Angle welds	$\gamma_{Mw} = 1.35$
	Weldings in first class	$\gamma_{Mw} = 1.05$
	Weldings in secondo class	$\gamma_{Mw} = 1.20$
FRICTION JOINTS	Ultimate Limit State	$\gamma_{Ms,ult} = 1.25$
	Serviceability Limit State	$\gamma_{Ms,ser} = 1.25$
	Ultimate Limit State (larger holes)	$\gamma_{Ms,ult} = 1.50$
FATIGUE	Fatice strength	$\gamma_{Mf} = 1.00$
FRAGILITY	Non welded	$\gamma_{C1} = 1.00$
	Welded	$\gamma_{C2} = 1.50$

### 2.8.2.1 Classification of steel cross sections

Behaviour of structural steel is ductile in behaviour since huge values of ultimate strain can be developed, namely in tension, after yielding. Nevertheless, slenderness of both section and member as a whole can undermine the natural ductility of steel as compression arises. Since, the above discussion mainly focused upon the global buckling issue, the present section will address the aspects related to local buckling of steel members which hugely affects their flexural behaviour. In particular, four different classes of profiles can be defined looking after their behaviour in terms of sectional strength and ductility, qualitatively depicted in Figure 2.14 in terms of moment-curvature relationships.

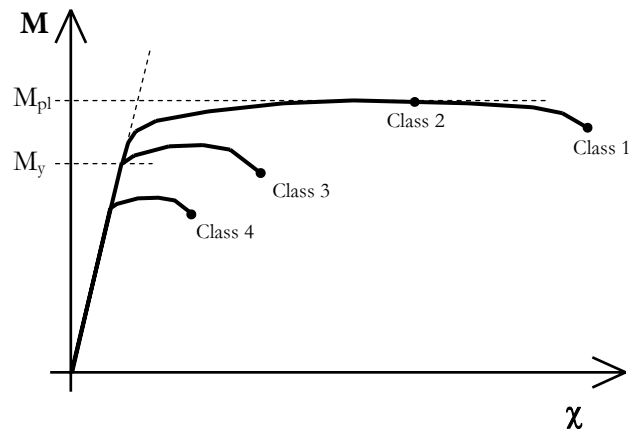


Figure 2.14: Possible moment-curvature behaviour for steel profiles.

In particular, the four classes corresponding to the various responses represented in the mentioned figure will be defined as follows:

- Class 1 cross-sections are those can form a plastic hinge with the rotation capacity required for plastic analysis;
- Class 2 cross-sections are those which can develop their plastic moment resistance, but have limited rotation capacity;
- Class 3 cross-section are those in which the calculated stress in the extreme compression fibre of the steel member can reach its yield stress, but local buckling is liable to prevent development of the plastic moment resistance;
- Class 4 cross-sections are those in which local buckling will occur before the attainment of yield stress in one or more parts of the cross-sections.

Beam-column sections can be classified into one of the above classes depending upon the three aspects listed below:

- effective length-to-thickness  $d/t$  of web and free length-to-thickness  $b/t$  of flanges;
- state of stress (pure bending, pure compression or bending and compression);
- grade of steel, being stronger steels more sensitive to local buckling phenomenon than weaker ones.

Table 2.3 summarizes the above concepts with reference to the most common hot-rolled I-shaped sections; similar tables can be found in EC3 for other joist sections.

Table 2.3: Classification of sections for local buckling according to EC3: webs.

Internal compression elements						
				<p>Axis of bending</p>		
Class	Element subject to bending	Element subject to compression	Element subject to bending and compression			
1	$c/t \leq 72\epsilon$	$c/t \leq 33\epsilon$	when $\alpha > 0,5$ : $c/t \leq \frac{396\epsilon}{13\alpha - 1}$ when $\alpha \leq 0,5$ : $c/t \leq \frac{36\epsilon}{\alpha}$			
2	$c/t \leq 83\epsilon$	$c/t \leq 38\epsilon$	when $\alpha > 0,5$ : $c/t \leq \frac{456\epsilon}{13\alpha - 1}$ when $\alpha \leq 0,5$ : $c/t \leq \frac{41,5\epsilon}{\alpha}$			
3	$c/t \leq 124\epsilon$	$c/t \leq 42\epsilon$	when $\psi > -1$ : $c/t \leq \frac{42\epsilon}{0,67 + 0,33\psi}$ when $\psi \leq -1$ : $c/t \leq 62\epsilon(1 - \psi)\sqrt{(-\psi)}$			
$\epsilon = \sqrt{235/f_y}$	$f_y$	235	275	355	420	460
	$\epsilon$	1,00	0,92	0,81	0,75	0,71

Table 2.4: Classification of sections for local buckling according to EC3: flanges.

Outstand flanges						
Rolled sections			Welded sections			
Class	Element subject to compression	Element subject to bending and compression				
		Tip in compression		Tip in tension		
Stress distribution in elements (compression positive)						
1	$c/t \leq 9\epsilon$	$c/t \leq \frac{9\epsilon}{\alpha}$	$c/t \leq \frac{9\epsilon}{\alpha\sqrt{\alpha}}$	$c/t \leq \frac{9\epsilon}{\alpha\sqrt{\alpha}}$	$c/t \leq \frac{9\epsilon}{\alpha\sqrt{\alpha}}$	$c/t \leq \frac{9\epsilon}{\alpha\sqrt{\alpha}}$
2	$c/t \leq 10\epsilon$	$c/t \leq \frac{10\epsilon}{\alpha}$	$c/t \leq \frac{10\epsilon}{\alpha\sqrt{\alpha}}$	$c/t \leq \frac{10\epsilon}{\alpha\sqrt{\alpha}}$	$c/t \leq \frac{10\epsilon}{\alpha\sqrt{\alpha}}$	$c/t \leq \frac{10\epsilon}{\alpha\sqrt{\alpha}}$
Stress distribution in elements (compression positive)						
3	$c/t \leq 14\epsilon$	$c/t \leq 21\epsilon\sqrt{k_\sigma}$ For $k_\sigma$ see Part 1-5				
$\epsilon = \sqrt{235/f_y}$	$f_y$	235	275	355	420	460
	$\epsilon$	1,00	0,92	0,81	0,75	0,71

The web and the flanges of the section can be classified according to their dimensions, the steel grade and the state of stress according to the rules briefly reported in Table 2.3 and Table 2.4. The section as a whole has to be classified in class of the most slender of its members. If such a section falls in Class 4, local stability occurs before of yielding moment and, consequently, the flexural strength of the member cannot be completely developed. For this reason an effective section have to be determined by reducing the compressed area of web and flange in order to obtain a reduced virtual section to be considered in both strength and stability check. The way in which such section can be determined are not completely explained within this notes for the sake of brevity; nevertheless, the reader could directly refer to Eurocode 3 (section 6.2.2.5) for this topic.

### 2.8.2.2 Stability check under axial load

Stability check under axial load can be carried out through the following inequality:

$$N_{Sd} \leq N_{Rd} = \chi_{\min} \beta_A A \frac{f_{ay}}{\gamma_{M1}}, \quad (2.72)$$

being  $\chi_{\min} = \min(\chi(\bar{\lambda}_x); \chi(\bar{\lambda}_y))$  a reduction factor related to the relative slenderness  $\bar{\lambda}$  defined as follows:

$$\bar{\lambda} = \sqrt{\frac{\beta_A A f_y}{N_{cr}}}. \quad (2.73)$$

The factor  $\beta_A$  is defined as a ratio between the effective area and the gross section area; for section belonging to the first three classes defined above  $\beta_A = 1$ , while values smaller than the unity characterize profiles in class 4. Further details about the definition of the effective area for Class 4 profiles will be given in the following. If  $\beta_A = 1$ , the following relationship can be stated between the relative slenderness  $\bar{\lambda}$ , the absolute one  $\lambda$  and the critical one  $\lambda_p$ :

$$\bar{\lambda} = \sqrt{\frac{A f_y}{\pi^2 EI} \cdot L_0^2} = \sqrt{\frac{f_y}{\pi^2 E} \cdot \frac{L_0^2}{\rho^2}} = \frac{\lambda}{\lambda_p} \quad (2.74)$$

Under a conceptual standpoint the parameter  $\chi$  is basically the inverse of the  $\omega$  factor reducing plastic strength of the section for looking after the global slenderness  $\lambda$  on the column. The relationship  $\omega(\bar{\lambda})$  depends once more by the kind of imperfections and, consequently, by the type of profile. Four curves denoted as *a*, *b*, *c* and *d* can be utilized for that relationship:

- Curve a represents quasi perfect shapes: hot-rolled I-sections ( $h/b > 1,2$ ) with thin flanges ( $t_f \leq 40\text{mm}$ ) if buckling is perpendicular to the major axis; it also represents hot-rolled hollow sections;
- Curve b represents shapes with medium imperfections: it defines the behaviour of most welded box-sections; of hot-rolled I-sections buckling about the minor axis; of welded I-sections with thin flanges ( $t_f > 40\text{mm}$ ) and of the rolled I-sections with medium flanges ( $40 < t_f \leq 100\text{mm}$ ) if buckling is about the major axis; it also concerns cold-formed hollow sections where the average strength of the member after forming is used;
- Curve c represents shapes with a lot of imperfections: U, L, and T shaped sections are in this category as are thick welded box-sections; cold-formed hollow sections designed to the yield strength of the original sheet; hot-rolled H-sections ( $h/b \leq 1,2$  and  $t_f \leq 100\text{mm}$ ) buckling about the minor axis; and some welded I-sections ( $t_f \leq 40\text{mm}$  buckling about the minor axis and  $t_f > 40\text{mm}$  buckling about the major axis);
- Curve d represents shapes with maximum imperfections: it is to be used for hot-rolled I-sections with very thick flanges ( $t_f > 100\text{ mm}$ ) and thick welded I-sections ( $t_f > 40\text{ mm}$ ), if buckling occurs in the minor axis.

Figure 2.15 shows how to choose the right curve for each shape and bending direction according to the properties mentioned above.

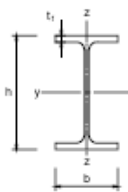
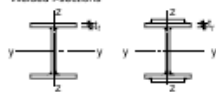
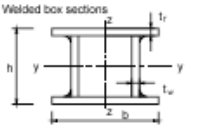
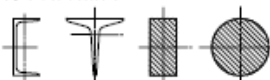
Cross-section	Limits	Buckling about axis	Buckling curve	
			S 235 S 275 S 355 S 420	S 460
 Rolled I-sections	$h/b > 1,2$ $t_f \leq 40\text{mm}$	y - y z - z	a b	a <sub>1</sub> a <sub>2</sub>
	$40\text{mm} < t_f \leq 100\text{mm}$	y - y z - z	b c	a a
		y - y z - z	b c	a a
	$h/b \leq 1,2$ $t_f \leq 100\text{mm}$	y - y z - z	b c	a a
y - y z - z		d d	c c	
 Welded I-sections	$t_f \leq 40\text{mm}$	y - y z - z	b c	b c
	$t_f > 40\text{mm}$	y - y z - z	c d	c d
 Hollow sections	hot rolled	any	a	a <sub>1</sub>
	cold formed	any	c	c
 Welded box sections	generally (except as below)	any	b	b
	thick welds: $a > 0,5 t_f$ $b/t_f < 30$ $h/t_{w} < 30$	any	c	c
 U, T-and solid sections		any	c	c
 L-sections		any	b	b

Figure 2.15: Stability curves for the various kinds of profiles.

Once the right curve has been chosen the value of  $\chi$  can be determined; different curve have to be used for determining the corresponding  $\chi$  values with reference to the two principal axis of the section.

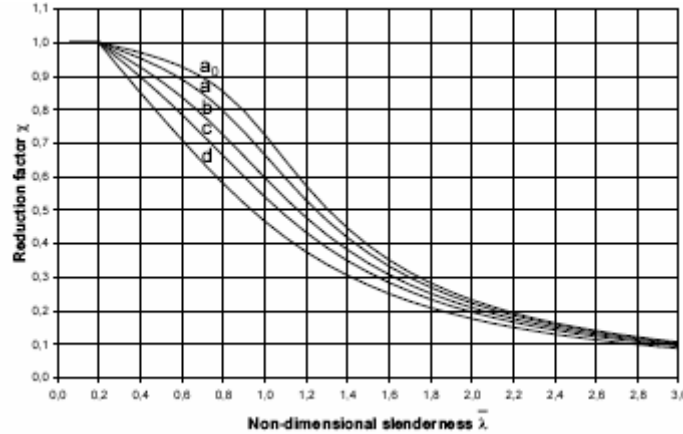


Figure 2.16: Stability curves according to EC3.

The curves in Figure 2.16 can be defined by the following general relationship in terms of the non-dimensional slenderness defined by equation (2.73):

$$\chi = \frac{1}{\Phi + \sqrt{\Phi^2 - \bar{\lambda}^2}} \leq 1.0, \quad (2.75)$$

with

$$\Phi = 0.5 \cdot \left[ 1 + \alpha \cdot (\bar{\lambda} - 0.2) + \bar{\lambda}^2 \right]. \quad (2.76)$$

The parameter  $\alpha$  is related to the level of imperfection affecting the structural member; since four curves have been introduced for describing the various kinds of imperfections, four values of  $\alpha$  have to be considered, each one for the corresponding stability curve (Table 2.1).

Table 2.5: Imperfection factors for buckling curves.

Buckling curve	a <sub>0</sub>	a	b	c	d
Imperfection factor $\alpha$	0,13	0,21	0,34	0,49	0,76

### 2.8.2.3 Stability check under eccentric axial load

Since there slight differences exist between the method for stability check of members under eccentric loads according to the ENV version [7] and the final EN one [14], both procedures will be proposed in the following. Indeed, while the first one is not yet valid, in the authors' opinion, is fitter for grasping the mechanical meaning of the various terms whose final EN formalization seems only formally more complicated. Moreover, since in the symbols adopted within the Eurocodes,  $y$  and  $z$  are the two principal axes of inertia, this choice will be assumed in the following sections.

#### 2.8.2.3.1 ENV 1-1-1993 [13] procedure.

Different formulae are provided depending on the class of the cross section. If it belongs to Classes 1 or 2 the following relationship, conceptually close to the one in equation (2.67) has to be considered:

$$\frac{N_{Sd}}{\chi_{\min} A f_{ay}} + \frac{k_y M_{y,Sd}}{\gamma_{M1} W_{pl,y} f_{ay}} + \frac{k_z M_{z,Sd}}{\gamma_{M1} W_{pl,z} f_{ay}} \leq 1, \quad (2.77)$$

where the coefficient  $\chi_{\min} = \min(\chi(\bar{\lambda}_y); \chi(\bar{\lambda}_z))$  can be evaluated according to the above remarks. Plastic moduli  $W_{pl,y}$  and  $W_{pl,z}$  are considered since plastic bending moment can be completely developed in

class 1 and 2 profiles. Second-order effects and the shape of diagram are considered through the factors  $k_y$  and  $k_{\psi}$ , the first of which is defined as follows:

$$k_y = 1 - \frac{\mu_y N_{Sd}}{\chi_y A f_{ay}}, \quad (2.78)$$

and

$$\mu_y = \bar{\lambda}_y \cdot (2\beta_{My} - 4) + \frac{W_{pl,y} - W_{el,y}}{W_{el,y}}, \quad (2.79)$$

and, finally, the value of  $\beta_M$  accounts for the shape of bending moments and can be deduced by Figure 2.17.

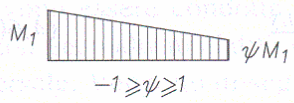
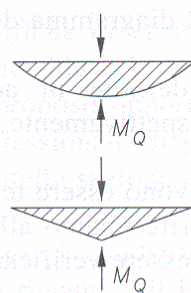
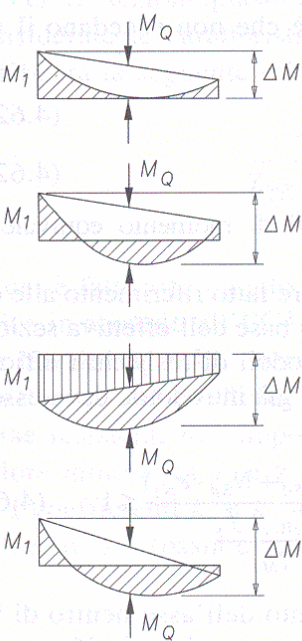
Bending Moment Diagram	Equivalent Uniform Moment Coefficient $\beta_M$
	$\beta_{M,\psi} = 1,8 - 0,7 \psi$
	$\beta_{M,Q} = 1,3$ $\beta_{M,Q} = 1,4$
	$\beta_M = \beta_{M,\psi} + \frac{M_Q}{\Delta M} (\beta_{M,Q} - \beta_{M,\psi})$ $M_Q =  \max M  \quad \text{Lateral load contribution only}$ $\Delta M = \begin{cases}  \max M  & \text{No sign change in bending moment} \\  \max M  +  \min M  & \text{Bending moments with variable sign} \end{cases}$

Figure 2.17:  $\beta_M$  factors depending on the shape of bending moment diagram.

Stability check of beam columns in class 3 can be carried out by simply substituting the plastic moduli with the elastic ones in equations from (2.77) to (2.79). Finally, for slender sections (Class 4) the relevant properties (area and strength moduli) of the effective section have to be evaluated and the bending moments need to be updated for taking into account the eccentricities  $e_{N,x}$  and  $e_{N,y}$  between the original centroid and the one of the effective section:

$$M_{y,Sd,eff} = M_{y,Sd} + N_{y,Sd} \cdot e_{Ny} \quad (2.80)$$

### 2.8.2.3.2 EN 1-1-1993 [14] procedure.

Few formal variations has been introduced in the final version of the Eurocode accepted as EN. In particular, a general expression for the stability check of beam-columns is proposed in the following form:

$$\frac{\frac{N_{Sd}}{\chi_y N_{Rk}} + k_{yy} \frac{M_{y,Sd} + N_{Ed} e_{Ny}}{\chi_y M_{y,Rk}}}{\gamma_{M1}} + k_{y\bar{z}} \frac{M_{\bar{z},Sd} + N_{Ed} e_{N\bar{z}}}{\chi_y M_{\bar{z},Rk}} \leq 1$$

$$\frac{\frac{N_{Sd}}{\chi_{\bar{z}} N_{Rk}} + k_{\bar{z}y} \frac{M_{y,Sd} + N_{Ed} e_{Ny}}{\chi_y M_{y,Rk}}}{\gamma_{M1}} + k_{\bar{z}\bar{z}} \frac{M_{\bar{z},Sd} + N_{Ed} e_{N\bar{z}}}{\chi_y M_{\bar{z},Rk}} \leq 1 \quad (2.81)$$

provided that no lateral-torsional buckling phenomena (which will be addressed in the 4th chapter) exist.

The values of  $N_{Rk}$ ,  $M_{y,Rk}$  and  $M_{\bar{z},Rk}$  are defined in the following general form:

$$N_{Rk} = A_i f_{ay} \quad (2.82)$$

$$M_{y,Rk} = W_y f_{ay} \quad M_{\bar{z},Rk} = W_{\bar{z}} f_{ay} \quad (2.83)$$

The geometrical properties reported in equations (2.82) and (2.83) can be assumed depending on the class of the transverse section as briefly summarized in Table 2.6.

Table 2.6: Values of geometrical properties depending of class section.

Class	1	2	3	4
$A_i$	A	A	A	$A_{eff}$
$W_y$	$W_{pl,y}$	$W_{pl,y}$	$W_{el,y}$	$W_{eff,y}$
$W_z$	$W_{pl,z}$	$W_{pl,z}$	$W_{el,z}$	$W_{eff,z}$

No substantial differences exist among the aspects described above. Nevertheless, as one compare equation (2.77) (and the corresponding ones for sections in class 3 or 4) with equation (2.81) can easily observe the key difference between the two approaches. In fact, four interaction factors  $k_{ij}$  (rather than two) are involved in equation (2.81) meaning that the bending contribution is different in the cases of buckling occurring either in  $y$  or  $\bar{z}$  direction.

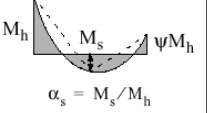
Table 2.7: Interaction factors according to Method 2 – Annex B [14].

Interaction factors	Type of sections	Design assumptions	
		elastic cross-sectional properties class 3, class 4	plastic cross-sectional properties class 1, class 2
$k_{yy}$	I-sections RHS-sections	$C_{my} \left( 1 + 0,6\bar{\lambda}_y \frac{N_{Ed}}{\chi_y N_{Rk} / \gamma_{M1}} \right)$ $\leq C_{my} \left( 1 + 0,6 \frac{N_{Ed}}{\chi_y N_{Rk} / \gamma_{M1}} \right)$	$C_{my} \left( 1 + (\bar{\lambda}_y - 0,2) \frac{N_{Ed}}{\chi_y N_{Rk} / \gamma_{M1}} \right)$ $\leq C_{my} \left( 1 + 0,8 \frac{N_{Ed}}{\chi_y N_{Rk} / \gamma_{M1}} \right)$
$k_{yz}$	I-sections RHS-sections	$k_{zz}$	$0,6 k_{zz}$
$k_{zy}$	I-sections RHS-sections	$0,8 k_{yy}$	$0,6 k_{yy}$
$k_{zz}$	I-sections	$C_{mz} \left( 1 + 0,6\bar{\lambda}_z \frac{N_{Ed}}{\chi_z N_{Rk} / \gamma_{M1}} \right)$ $\leq C_{mz} \left( 1 + 0,6 \frac{N_{Ed}}{\chi_z N_{Rk} / \gamma_{M1}} \right)$	$C_{mz} \left( 1 + (2\bar{\lambda}_z - 0,6) \frac{N_{Ed}}{\chi_z N_{Rk} / \gamma_{M1}} \right)$ $\leq C_{mz} \left( 1 + 1,4 \frac{N_{Ed}}{\chi_z N_{Rk} / \gamma_{M1}} \right)$
	RHS-sections		$C_{mz} \left( 1 + (\bar{\lambda}_z - 0,2) \frac{N_{Ed}}{\chi_z N_{Rk} / \gamma_{M1}} \right)$ $\leq C_{mz} \left( 1 + 0,8 \frac{N_{Ed}}{\chi_z N_{Rk} / \gamma_{M1}} \right)$

For I- and H-sections and rectangular hollow sections under axial compression and uniaxial bending  $M_{y,Ed}$  the coefficient  $k_{zy}$  may be  $k_{zy} = 0$ .

Two alternative approaches are reported in EC3 [14] for determining the values of such factors; they are reported in two different annexes at the same document. Only the so-called “Method 2” reported in Annex B is explicitly reported herein for the sake of brevity; its formulation for the case in which members are not susceptible of lateral-torsional buckling is summarized in Table 2.7. Finally, Table 2.8 summarized how the equivalent uniform moment factors have to be evaluated according to the mentioned Method 2.

Table 2.8: Equivalent uniform moment factors according to Method 2 – Annex B [14].

Moment diagram	range		$C_{my}$ and $C_{mz}$ and $C_{mLT}$	
			uniform loading	concentrated load
	$-1 \leq \psi \leq 1$		$0,6 + 0,4\psi \geq 0,4$	
 $\alpha_s = M_s / M_h$	$0 \leq \alpha_s \leq 1$	$-1 \leq \psi \leq 1$	$0,2 + 0,8\alpha_s \geq 0,4$	$0,2 + 0,8\alpha_s \geq 0,4$
	$-1 \leq \alpha_s < 0$	$0 \leq \psi \leq 1$	$0,1 - 0,8\alpha_s \geq 0,4$	$-0,8\alpha_s \geq 0,4$
		$-1 \leq \psi < 0$	$0,1(1-\psi) - 0,8\alpha_s \geq 0,4$	$0,2(-\psi) - 0,8\alpha_s \geq 0,4$
 $\alpha_h = M_h / M_s$	$0 \leq \alpha_h \leq 1$	$-1 \leq \psi \leq 1$	$0,95 + 0,05\alpha_h$	$0,90 + 0,10\alpha_h$
	$-1 \leq \alpha_h < 0$	$0 \leq \psi \leq 1$	$0,95 + 0,05\alpha_h$	$0,90 + 0,10\alpha_h$
		$-1 \leq \psi < 0$	$0,95 + 0,05\alpha_h(1+2\psi)$	$0,90 - 0,10\alpha_h(1+2\psi)$

For members with sway buckling mode the equivalent uniform moment factor should be taken  $C_{my} = 0,9$  or  $C_{Mz} = 0,9$  respectively.

$C_{my}$ ,  $C_{mz}$  and  $C_{mLT}$  should be obtained according to the bending moment diagram between the relevant braced points as follows:

moment factor	bending axis	points braced in direction
$C_{my}$	y-y	z-z
$C_{mz}$	z-z	y-y
$C_{mLT}$	V-V	V-V

## 2.9 Applications

Application of the above theory is proposed in the following. Some worked examples deal with the main topics covered by this section, while few unworked one are left to the reader.

### 2.9.1 Worked examples

Three worked examples dealing with the key topics discussed in the above sections are proposed in the following.

### 2.9.1.1 Euler load for a generally restrained beam-column

The first example deals with the evaluation of the Euler critical load for a generally restrained beam-column. In particular, flexible restraints are present at both ends and their flexibility is defined as follows:

$$\varepsilon_A = \frac{L_{col}}{10EI_{col}} , \quad (2.84)$$

$$\varepsilon_B = \frac{L_{col}}{5EI_{col}} . \quad (2.85)$$

being  $L_{col}=5.0$  m the member span length and  $I_{col}$  the moment of inertia of the transverse section with reference to an axis normal to the plane of possible buckling occurrence. The beam-column is represented in Figure 2.18; since it is a non-sway member equation (2.44) or the alignment chart in Figure 2.10a has to be used for evaluating the effective length  $L_0$  or, equivalently, the  $\beta$  coefficient to be adopted in equation (2.43).

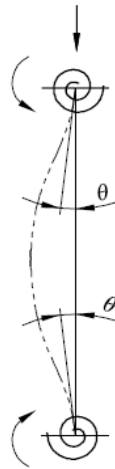


Figure 2.18: Structural scheme of the beam-column.

First of all, the values of the non-dimensional flexibilities  $k_A$  and  $k_B$  have to be determined according to their definition:

$$k_A = \frac{\varepsilon_A}{L_{col}/EI_{col}} = \frac{1}{10} = 0.10 , \quad (2.86)$$

$$k_B = \frac{\varepsilon_B}{L_{col}/EI_{col}} = \frac{1}{5} = 0.20 .$$

As a matter of principle, the corresponding value of the  $\beta$  coefficient is within the range  $[0.5, 1.0]$ , being the column a non-sway member. The equation (2.44) can be applied for determining its value:

$$\beta = 0.5 \cdot \sqrt{\left(1 + \frac{0.10}{0.45 + 0.10}\right) \cdot \left(1 + \frac{0.20}{0.45 + 0.20}\right)} = 0.622 . \quad (2.87)$$

The above value is rather conservative with respect to the one which could be derived by the alignment chart in figure Figure 2.10a, as desirable for an approximate formula.

### 2.9.1.2 Stability check of an axially loaded beam-column

Let us consider a member in compression whose transverse section is realized by a profile HE 200 B made out of steel S235. The overall span length of the member is 7.5 m and displacement in the direction perpendicular to the web plane constraints the displacements in that direction (Figure 2.19).

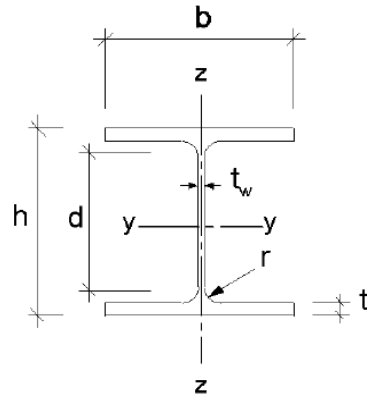


Figure 2.19: Beam-column under axial force.

The transverse section of the beam is characterized by the following geometrical parameters:

- depth	$h$	200 mm;
- width	$b$	200 mm;
- flange thickness	$t_f$	15 mm;
- web thickness	$t_w$	9 mm;
- radius	$r$	18 mm;
- area	$A$	$7810 \text{ mm}^2$ ;
- Moment of inertia with respect to the strong axis	$I_y$	$5696 \cdot 10^4 \text{ mm}^4$ ;
- Moment of inertia with respect to the weak axis	$I_z$	$2003 \cdot 10^4 \text{ mm}^4$ .

For the sake of brevity the exercise will be only solved with reference to the EC3 provisions for stability check.

Step #1: classification of the transverse section:

Since the adopted steel grade is  $f_y=235$  MPa the value  $\epsilon=1$  can be assumed for the parameter mentioned in Table 2.3 and Table 2.4. The following values of the length-to-thickness ratios can be evaluated for flange and web:

- flange	$c/t_f=(200/2)/15=6.7 \leq 10$	Class 1;
- web	$d/t_w=(200-2 \cdot 15-2 \cdot 18)/9=14.9 \leq 33$	Class 1

Finally, the profile HE200B made out of steel S235 is in class 1 if loaded in compression.

Step #2.1: evaluating the (elastic) Euler load for buckling along the strong axis:

Since hinged restraints can be recognized for both ends and no further constraints control displacements in the mentioned direction, the effective length  $L_{0,y}$  is equal to the nominal one ( $L=7500$  mm) and the Euler load can be easily derived:

$$N_{\sigma,y} = \frac{\pi^2 EI_y}{L_{0,y}^2} = \frac{\pi^2 210000 \cdot 56960000}{7500^2} = 2098.78 \text{ kN} . \quad (2.88)$$

Step #2.2: evaluating relative (non-dimensional) slenderness along the strong axis:

$$\bar{\lambda}_y = \sqrt{\frac{\beta_A A f_{ay}}{N_{\sigma,y}}} = \sqrt{\frac{1 \cdot 7810 \cdot 235}{2098.78 \cdot 10^3}} = 0.935 . \quad (2.89)$$

Step #2.3: determination of the reduction factor  $\chi_y$ :

According to Figure 2.15 the profile follows the *curve b* and, consequently, the following value of the reduction factor  $\chi_y$  can be evaluated:

$$\Phi_y = 0.5 \cdot \left[ 1 + \alpha \cdot (\bar{\lambda}_y - 0.2) + \bar{\lambda}_y^2 \right] = 0.5 \cdot \left[ 1 + 0.34 \cdot (0.935 - 0.2) + 0.935^2 \right] = 1.062 , \quad (2.90)$$

and

$$\chi_y = \frac{1}{\Phi_y + \sqrt{\Phi_y^2 - \bar{\lambda}_y^2}} = \frac{1}{1.062 + \sqrt{1.062^2 - 0.935^2}} = 0.6387 . \quad (2.91)$$

Step #3.1: evaluating the (elastic) Euler load for buckling along the weak axis:

Since transverse displacements are constrained at mid-span, the effective length  $L_{0,\zeta}$  is one half of the nominal one ( $L=7500$  mm) and the Euler load can be easily derived:

$$N_{cr,\zeta} = \frac{\pi^2 EI_{\zeta}}{L_{0,\zeta}^2} = \frac{\pi^2 210000 \cdot 20030000}{3250^2} = 2952.10 \text{ kN} . \quad (2.92)$$

Step #3.2: evaluating relative (non-dimensional) slenderness along the weak axis:

$$\bar{\lambda}_{\zeta} = \sqrt{\frac{\beta_A A f_{ay}}{N_{cr,\zeta}}} = \sqrt{\frac{1 \cdot 7810 \cdot 235}{2952.1 \cdot 10^3}} = 0.788 . \quad (2.93)$$

Step #3.3: determination of the reduction factor  $\chi_{\zeta}$ :

According to Figure 2.15 the profile follows the *curve c* and, consequently, the following value of the reduction factor  $\chi_{\zeta}$  can be evaluated:

$$\Phi_{\zeta} = 0.5 \cdot \left[ 1 + \alpha \cdot (\bar{\lambda}_{\zeta} - 0.2) + \bar{\lambda}_{\zeta}^2 \right] = 0.5 \cdot \left[ 1 + 0.49 \cdot (0.788 - 0.2) + 0.788^2 \right] = 0.955 , \quad (2.94)$$

and

$$\chi_{\zeta} = \frac{1}{\Phi_{\zeta} + \sqrt{\Phi_{\zeta}^2 - \bar{\lambda}_{\zeta}^2}} = \frac{1}{0.955 + \sqrt{0.955^2 - 0.788^2}} = 0.6695 . \quad (2.95)$$

Step #4: evaluating the ultimate axial load capacity:

The minimum value of the reduction factor evaluated along the two directions has to be considered for determining the ultimate bearing capacity of the member.

$$N_{b,Rd} = \chi_{\min} \beta_A A \frac{f_{ay}}{\gamma_{M1}} = 0.6387 \cdot 7810 \cdot \frac{235}{1.05} = 1116.4 \text{ kN} . \quad (2.96)$$

### 2.9.1.3 Stability check of an eccentrically loaded beam-column

The beam-column represented in Figure 2.20 has the same transverse section described in the previous example. Transverse displacements are constrained at the top of the column since the two following values of the  $\beta$  coefficient can be assumed:

- buckling in the strong direction (perpendicular to  $y$  axis)  $\beta_y = 2.0$ ;
- buckling in the weak direction (perpendicular to  $\zeta$  axis)  $\beta_z = 1.0$ ;

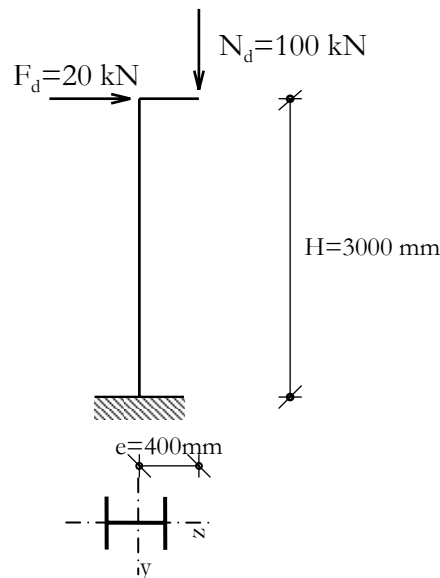


Figure 2.20: Beam-column under eccentric axial force.

Step #1: classification of the transverse section:

According to the findings of the previous exercise, the profile HE200B made out of steel S235 is in class 1 if loaded in compression.

Step #2.1: evaluating the (elastic) Euler load for buckling along the strong axis:

Since hinged restraints can be recognized for both ends and no further constraints control displacements in the mentioned direction, the effective length  $L_{e,y}$  is equal to the nominal one ( $L=7500$  mm) and the Euler load can be easily derived:

$$N_{e,y} = \frac{\pi^2 EI_y}{L_{e,y}^2} = \frac{\pi^2 210000 \cdot 56960000}{6000^2} = 3279.15 \text{ kN} \quad \square \quad (2.97)$$

Step #2.2: evaluating relative (non-dimensional) slenderness along the strong axis:

$$\bar{\lambda}_y = \sqrt{\frac{\beta_A A f_{yk}}{N_{e,y}}} = \sqrt{\frac{1 \cdot 7810 \cdot 235}{3279.15 \cdot 10^3}} = 0.748 \quad \square \quad (2.98)$$

Step #2.3: determination of the reduction factor  $\chi_y$ :

According to Figure 2.15 the profile follows the *α* *ω* *ω* *β* and, consequently, the following value of the reduction factor  $\chi_y$  can be evaluated:

$$\Phi_y = 0.5 \cdot [1 + \alpha \cdot (\bar{\lambda}_y - 0.2) + \bar{\lambda}_y^2] = 0.5 \cdot [1 + 0.34 \cdot (0.748 - 0.2) + 0.748^2] = 0.873 \quad \square \quad (2.99)$$

and

$$\chi_y = \frac{1}{\Phi_y + \sqrt{\Phi_y^2 - \bar{\lambda}_y^2}} = \frac{1}{0.873 + \sqrt{0.873^2 - 0.748^2}} = 0.7559 \quad \square \quad (2.100)$$

Step #3: evaluation of the relevant interaction factors:

Since no bending moment is applied around the z-axis the only interaction factor to be determined for applying the first one of the two equations (2.69) is the term  $k_{zy}$ . Linear variation can be observed for the bending moment around y-axis, which varies from the two following values:

- $M_{y,Ed,op} = N_{Ed} \cdot e = 100 \cdot 0.40 = 40 \text{ kNm}$ ;
- $M_{y,Ed,max} = N_{Ed} \cdot e + F_{Ed} \cdot H = 100 \cdot 0.40 + 20 \cdot 3.0 = 100 \text{ kNm}$ ;

Consequently, the maximum moment to be considered in equation (2.69) is  $M_{y,Ed} = 100 \text{ kNm}$  and, according to Table 2.8 the following value can be assumed for the equivalent uniform moment factor  $C_{my}$ :

$$\psi = \frac{M_{y,Ed,op}}{M_{y,Ed,max}} = \frac{40}{100} = 0.40 \Rightarrow C_{my} = 0.6 + 0.4\psi = 0.76 \quad \square \quad (2.101)$$

Finally, the value of the interaction factor  $k_{zy}$  can be derived according to the formulae reported in the first row of Table 2.7, provided that  $\bar{\lambda}_y < 1.0$ :

$$k_{zy} = C_{my} \cdot \left[ 1 + (\bar{\lambda}_y - 0.2) \cdot \frac{N_{Ed}}{\chi_y A f_{yk} / \gamma_{M1}} \right] = 0.76 \cdot \left[ 1 + (0.748 - 0.2) \cdot \frac{100000}{0.748 \cdot 7810 \cdot 235 / 1.05} \right] = 1.042 \quad \square \quad (2.102)$$

||

Step #4.1: evaluating the (elastic) Euler load for buckling along the weak axis:

Since transverse displacements are constrained at mid-span, the effective length  $L_{e,z}$  is one half of the nominal one ( $H=6000$  mm) and the Euler load can be easily derived:

$$N_{e,z} = \frac{\pi^2 EI_z}{L_{e,z}^2} = \frac{\pi^2 210000 \cdot 20030000}{3000^2} = 4612.45 \text{ kN} \quad \square \quad (2.103)$$

Step #4.2: evaluating relative (non-dimensional) slenderness along the weak axis:

$$\bar{\lambda}_z = \sqrt{\frac{\beta_A A f_{yk}}{N_{e,z}}} = \sqrt{\frac{1 \cdot 7810 \cdot 235}{4612.45 \cdot 10^3}} = 0.631 \quad \square \quad (2.104)$$

Step #4.3: determination of the reduction factor  $\chi_z$ :

According to Figure 2.15 the profile follows the *α* *ω* *ω* *ε* and, consequently, the following value of the reduction factor  $\chi_z$  can be evaluated:

$$\Phi_z = 0.5 \cdot [1 + \alpha \cdot (\bar{\lambda}_z - 0.2) + \bar{\lambda}_z^2] = 0.5 \cdot [1 + 0.49 \cdot (0.631 - 0.2) + 0.631^2] = 0.805 \quad \square \quad (2.105)$$

and

$$\chi_{\kappa} = \frac{1}{\Phi_{\kappa} + \sqrt{\Phi_{\kappa}^2 - \bar{\lambda}_{\kappa}^2}} = \frac{1}{0.805 + \sqrt{0.805^2 - 0.631^2}} = 0.7664 \quad . \quad (2.106)$$

Step #5: evaluation of the relevant interaction factors:

Since no bending moment is applied around the z-axis the only interaction factor to be determined for applying the second one of the two equations (2.69) is the term  $k_{zy}$ . An easy relationship is stated for determining this factor as a function of  $k_{yy}$  as follows:

$$k_{zy} = 0.6k_{yy} = 0.625 \quad . \quad (2.107)$$

Step #6: final stability check:

The two equations (2.69) can be finally applied for checking the given structure against global buckling:

$$\begin{aligned} \frac{100000}{0.7559 \cdot 7810 \cdot 235} + 1.042 \cdot \frac{100000000}{0.7559 \cdot 56960000 \cdot 235} &= 0.076 + 0.011 = 0.087 \leq 1 \\ \frac{100000}{0.7664 \cdot 7810 \cdot 235} + 0.625 \cdot \frac{100000000}{0.7664 \cdot 20030000 \cdot 235} &= 0.075 + 0.018 = 0.093 \leq 1 \end{aligned} \quad . \quad (2.108)$$

## 2.9.2 Unworked examples

The following exercises are left to the readers:

- 1) for the same beam-column reported in paragraph 2.9.1.1, evaluate the  $\beta$  coefficient in the case of sway member. Compare the results obtained by the simplified formula and the alignment chart;
- 2) for the same beam-column described in paragraph 2.9.1.2, evaluate the ultimate load bearing capacity according to the Italian Code;
- 3) for the same beam-column described in paragraph 2.9.1.2, evaluate the ultimate load bearing capacity considering a steel grade s355;
- 4) for the same beam-column described in paragraph 2.9.1.3, evaluate the maximum lateral load  $F_{Sd,max}$  with reference to the global stability check of the structure;
- 5) for the same beam-column described in paragraph 2.9.1.3, perform the stability check according to the Italian code.